Bayesian Linearized Seismic Inversion with Locally Varying Anisotropy

E. L. Bongajum, J. Boisvert and M. D. Sacchi

Inversion of seismic data is commonly used in the quantitative estimation of elastic properties of reservoirs. In some cases, the spatial variations of these elastic properties characterize geological formations that display nonlinear features such as channels or folds with complex spatial anisotropies. Consequently, single trace-based inversions are often used because it is difficult to impose spatial constrains in the inversion to provide geologically consistent estimates of the elastic parameters at the seismic scale. Locally varrying anisotropy (LVA) is incorporated in the Bayesian formulation of the inverse problem to impose such spatial constrains in the lateral continuity of the elastic properties. This favours a multiple trace-based inversion. The formulation uses covariances obtained through the quantitative modeling of the spatial statistics of the elastic parameters. The computation of spatial correlation uses anisotropic distances between locations within the geological formation. A synthetic validation of the method using a least squares approach shows an improvement in the inference of acoustic impedances from seismic data.

Introduction

Regularization methods, which can also be justified from a Bayesian perspective, used in the formulation of inverse problems are very popular (Oldenburg et al., 1983; Sacchi et al., 1998; Velis, 2009; Bosch, 2009). Although these methods allow for better estimation of the model ($\mathbf{m}$) that can adequately explain the geophysical data, implementing such methodology to geophysical inverse problems can be challenging. For example, in the inversion of seismic data for impedance, the solution is non unique due in part to the limited bandwidth of the seismic data. Moreover, the impedance models are invaluable to constrain the geostatistical simulations of porosity (Doyen, 1988).

Since the estimated model that fits the geophysical data often characterizes the spatial variation of a physical rock property within a target zone, one of the goals of inversion is for the model to fully capture the small, intermediate, and large scale fluctuations of these physical rock properties as depicted in well logs. While the terminology may be more familiar for geostatisticians, equivalent terms used by geophysicists include high, intermediate and low frequency information respectively. Considering that geophysical data are often sampled discretely in finite space or time, the model ($\mathbf{m}$) that explains the observed data is considered to be an element of a model space, and can be written as a vector:

$$\mathbf{m} = \begin{bmatrix} \mathrm{m}_1, \mathrm{m}_2, \ldots, \mathrm{m}_i, \ldots, \mathrm{m}_N \end{bmatrix}^{\mathbf{T}}$$

where the elements of the vector (m_i) represent the model parameters.

Nowadays, more advanced formulations are used such that seismic inversion combines geology, well logs, rock physics and geostatistics. Examples of applications that use rock physics relations to constrain seismic inversion include Bosch (2004) and Eidsvik et al. (2004). The idea of using geostatistics to condition the seismic inversion (geostatistical inversion) on the other hand was initially proposed by Haase and Dubrule (1994). The latter advocate for the geostatistical simulation process to be an integral part of the seismic inversion process. In the approach proposed by Haase and Dubrule (1994), the seismic data is used to constrain the inversion within the seismic bandwidth whereas the short scale information is constrained by the variograms obtained from the well logs. Consequently, geostatistics is important because it imposes true spatial constraints obtained from variograms especially for small scales that are not captured by the band-limited seismic data (Bosch et al., 2010). Torres-Verdin et al. (1999) demonstrate how geostatistical inversion can be applied for reservoir characterization. Other authors such as Pendrel and Van Riel (1997) used geostatistics differently whereby kriging is used to constrain the low frequency information of the acoustic impedance model that is not present within the seismic bandwidth.

Most of the inversion techniques are conducted on a trace by trace basis to estimate the model. Hence, emphasis is placed on the vertical variability estimated from variograms at the expense of the lateral variability. Eidsvik et al. (2004) use a Bayesian framework to formulate an amplitude variation with offset (AVO) inverse problem such that it incorporates lateral spatial continuity in the prior probability density through random markov field assumptions. Jensäs'(2008) approach is also set on the assumption of Markov properties whereby the inversion result on one trace is only dependent on the immediate neighbouring traces. In most of the inversion schemes of this category, one of the important consideration remains in carefully defining the directions of lateral continuity such that nonlinear geological continuities can be well captured. In this paper, we focus our investigation on using covariances that incorporate such information in the definition of the prior model. This can be done by considering locally varrying anisotropy (LVA) that helps to incorporate directional dependence in the geological continuity. Boisvert and Deutsch (2011) provide an application of geostatistical simulations with LVA where nonlinear distances used in the computation of the covariances are used to incorporate geological anisotropies. Anisotropy in the present context characterizes the aspect ratios in the scale lengths associated to the directions of maximum and minimum continuity.

In the following sections, a brief description of the Bayesian formulation of the inverse problem is first presented. This is followed by synthetic tests for acoustic seismic inversion where details on how the spatial correlations between the model parameters are incorporated in the inversion process are provided. The investigations use synthetic seismic data of different signal to noise ratios.

The Inverse problem

The Bayesian framework forms a general, consistent and convenient way of combining multiple model information in solving inverse problems. The fundamental ingredients required to formulate an inverse problem includes prior information of the model, observations (data) and the physical theory that relates the model parameters to the observed data. These can be combined to provide a posterior probability density that is given as

$$\sigma\left(\mathbf{m}\right) = cL\left(\mathbf{m}\right)\rho\left(\mathbf{m}\right)$$,

where $\sigma\left(\mathbf{m}\right)$ is the posterior density, c is a normalization constant, $L\left(\mathbf{m}\right)$ is the likelihood function and $\rho\left(\mathbf{m}\right)$ is the prior model density. A more explicit form of the above expression can be written as

$$\sigma\left(\mathbf{m}\right) = cL\left(\mathbf{d} \mid \mathbf{m}\right)\rho\left(\mathbf{m}\right),$$

with $\mathbf{d}$ being the data. In the real world, we are usually faced with the challenge of imperfect mathematical formulations to describe physical systems under study (modelization uncertainties) and noise. In this work, we assume the mathematical formulation of the physical theory to be exact and that the observed data consists of noise hence the notation $\mathbf{d}_{\mathrm{obs}}$ where

$$\mathbf{d}_{\mathrm{obs}} \approx \mathbf{g}\left(\mathbf{m}\right) + \mathbf{noise},$$

with $\mathbf{g}\left(\mathbf{m}\right)$ representing the mathematical formulation of the physical system under study. In other words, it is a function that maps the model parameters to the data space.

The main underlying challenge of the Bayesian approach resides on the choise of probability model adopted (Tarantola, 2005). $L\left(\mathbf{d} \mid \mathbf{m}\right)$ statistically characterizes predictions of observed data/measurements given the model parameters. In other words, it characterizes the misfit between predicted and observed data. Let us consider the misfit to be a Gaussian model where we have

$$L\left(\mathbf{d} \mid \mathbf{m}\right) = c_1 \exp\left[\frac{1}{2}\left(\mathbf{g}\left(\mathbf{m}\right) - \mathbf{d}_{\mathrm{obs}}\right)\mathbf{C}_{\mathrm{d}}^{-1}\left(\mathbf{g}\left(\mathbf{m}\right) - \mathbf{d}_{\mathrm{obs}}\right)\right],$$

with $\mathbf{C}_d$ representing a covariance matrix that characterizes the uncertainties in the observed data and c_1 as a normalization constant.

The prior model ($\rho(\mathbf{m})$) is the probability of the information obtained independently of the observed data. If we consider the model parameters to be part of a Gaussian random field, then it suffices to argue that the model parameters being investigated is a random realization of a Gaussian random field with a mean $\mathbf{m}_{prior}$. Thus, $\rho(\mathbf{m})$ maximizes the probability of the model $\mathbf{m}$ to be close to $\mathbf{m}_{prior}$ whereby

$$\rho(\mathbf{m}) = c_2 \exp\left[\frac{1}{2}\left(\mathbf{g}(\mathbf{m}) - \mathbf{d}_{obs}\right)\mathbf{C}_m^{-1}\left(\mathbf{g}(\mathbf{m}) - \mathbf{d}_{obs}\right)\right],$$

with c_2 as a normalization constant and $\mathbf{C}_m$ as the prior covariance matrix for the model parameters. $\mathbf{C}_m$ contains information that describes the correlation between the various model parameters.

Some authors that use the Gaussian model in describing $\rho(\mathbf{m})$ include Bosch (2004) and Buland and Omre (2003). On the hand, authors such as Sacchi et al. (1996) and Alemie and Sacchi (2011) show applications where a Cauchy model is used to describe $\rho(\mathbf{m})$ in order to obtain a sparse solution of an inverse problem.

The formulation of the posterior density in this work will also be Gaussian where the solution can be obtained by finding the maximum posterior model (MAP solution). This approach provides one solution in the least squares sense ("best estimate"). The underlying principle of the best estimate of the model parameters is such that the misfit between the observed data and estimates of the observed data are minimized. The minimization procedure of the data is constrained by other conditions defined within the formulation of the prior model. The posterior density is thus given as

$$\sigma(\mathbf{m}) = c \exp\left[J\right]$$

where,

$$J = \left[\frac{1}{2}\left(\mathbf{g}(\mathbf{m}) - \mathbf{d}_{obs}\right)\mathbf{C}_d^{-1}\left(\mathbf{g}(\mathbf{m}) - \mathbf{d}_{obs}\right)\right] + \left[\frac{1}{2}\left(\mathbf{m} - \mathbf{m}_{prior}\right)\mathbf{C}_m^{-1}\left(\mathbf{m} - \mathbf{m}_{prior}\right)\right]$$

represents the cost funtion to be minimized.

If the relation between the model parameters and the data is nonlinear, nonlinear optimization techniques which require an iterative approach to the solution can be adopted (e.g. Newton optimization method, Tarantola, 2005; Bosch, 2004). On the other hand, let us assume $\mathbf{g}(\mathbf{m})$ can be expressed as linear combination of the model parameters i.e. $\mathbf{g}(\mathbf{m}) = \mathbf{G}\mathbf{m}$. By equating the first order partial derivatives of J to zero, a simplified expression for $\mathbf{m}$ is given by

$$J\frac{\partial J}{\partial \mathbf{m}^{\mathrm{T}}} = \mathbf{G}^{\mathrm{T}}\mathbf{C}_d^{-1}\left(\mathbf{G}\mathbf{m} - \mathbf{d}_{obs}\right) + \mathbf{C}_m^{-1}\left(\mathbf{m} - \mathbf{m}_{prior}\right) = 0 \qquad (1)$$

$$\mathbf{m} = \left(\mathbf{I} + \mathbf{C}_m\mathbf{G}^{\mathrm{T}}\mathbf{C}_d^{-1}\mathbf{G}\right)^{-1}\left(\mathbf{m}_{prior} + \mathbf{C}_m\mathbf{G}^{\mathrm{T}}\mathbf{C}_d^{-1}\mathbf{d}_{obs}\right). \qquad (2)$$

Results and Discussion

a)   Example of Impedance prediction from Seismic Amplitude

The inverse problem is formulated such that the logarithm of the acoustic impedance $\mathbf{m} = \log\left(\mathbf{Z}_p\right)$ is the parameter of interest. Such a formulation allows for the use of a linear operator to convert impedance information to seismic amplitudes and hence the inversion procedure follows equation 2 where $\mathbf{G}$ is the product of a convolution matrix (*contains information of the source wavelet*) and a differential matrix. The covariance matrix $\mathbf{C}_m$ is based on the statistics of the logarithm of the impedance. The 2D synthetic data for the impedance model is derived from the wyllie transformation (Bosch, 2004) of a kriged 2D porosity (ϕ) model to which we added some gaussian noise in order to provide some deviation from the wyllie transformation (Figures 1 and 2). The 2D synthetic porosity model was derived by using an LVA field (Figure 2c), information at two well locations (Figure 3) and algorithms for kriging with LVA (Boisvert and Deutsch, 2011).

In performing the inversion, it is ideal to have a prior model that is close to the solution space. Often, information from the prior models can be obtained from the existing measurements of the model parameters of interest. In geophysics, petrophysical databases for velocities, densities, porosities as well as borehole logs can be valuable sources for such information. In the present study, synthetic tests are perfomed to determine impedance model from seismic data to which some band-limited noise has been added such that the signal to noise ratio (SNR) is 1 (Figures 4a & b). The zero-offset synthetic seismic amplitudes are obtained from the impedance model through the convolution process. The source waveform is a ricker wavelet with a dominant frequency of 50Hz. The prior model is based on the trend of $\mathbf{m}$ (mean).

The investigations have been designed to probe the impact of the structure of the model covariance matrix in the quality of the inversion results. The case studies considered are summarized below.

Case 1: Model parameters at each time sample are independent. This means $\mathbf{C}_m$ is a diagonal matrix. The diagonal terms are the variance, $\left(\sigma_m^2\right)$, of the model parameters. Knowledge of the standard deviation of the gaussian noise σ_n can also be used in the estimation of σ_m^2. The normal distribution of the noise causes the misfit in the seismic amplitudes,

$$J_1 = \left(\mathbf{g}\left(\mathbf{m}\right) - \mathbf{d}_{obs}\right)\mathbf{C}_d^{-1}\left(\mathbf{g}\left(\mathbf{m}\right) - \mathbf{d}_{obs}\right),$$

to reduce to a chi-square statistics. Consequently, the expected value, $E\left(J_1\right)$, will be N (number of trace samples).

Case 2: Assumes model parameters are coupled in the depth direction. This means the off-diagonal terms of $\mathbf{C}_m$ are non-zero. The elements of these matrices are obtained from parametric model fits to experimental variograms or covariances computed from well logs (Deutsch and Journel, 1998; Goff and Jordan, 1998). In this work, the synthetic well log coincides with the location of trace 5 (CDP = 5) in the 2D seismic data. The exponential model was used throughout this study. While the model parameters at a given trace location are considered to be coupled, the traces are considered to be independent of each other. If there are N samples per trace, then the covariance matrix is an $MN \times MN$ matrix with $M = 1$,

$$\mathbf{C}_m = \mathbf{C}_{(i,i)} = \begin{pmatrix} c_{11} & \cdots & c_{1N} \\ \vdots & \ddots & \vdots \\ c_{1N} & \cdots & c_{NN} \end{pmatrix},$$

where c_{jk} represent the covariance between the model parameters at time samples j and k in trace i.

Case 3: Assume the model parameters are coupled in the vertical and lateral direction. The crosscovariance between neighbouring traces is also included in the covariance matrix which allows for multiple traces to be inverted at once $(M>1)$. The covariance between any two points takes in to account a geometric anisotropy of 0.01 in the ranges (Deutsch and Journel, 1998; Goovaerts, 1997). The major direction of continuity is horizontal (along direction of increasing CDP number). The model covariance becomes a composite matrix with fundamental building blocks of $N \times N$ covariance matrices $\mathbf{C}_{(i,j)}$:

$$\mathbf{C}_m = = \begin{pmatrix} \mathbf{C}_{(1,1)} & \cdots & \mathbf{C}_{(1,M)} \\ \vdots & \ddots & \vdots \\ \mathbf{C}_{(M,1)} & \cdots & \mathbf{C}_{(M,M)} \end{pmatrix} \text{ where the subscripts represent pairs of trace numbers.}$$

Case 4: Unlike Case 3, the computation of the covariance is conditioned by information of the LVA field whereby two points in space are related by the path with the minimum anisotropic distance. Boisvert and Deutsch (2011) provide further details of how such a model covariance matrix can be computed. Background information of the LVA field can either be acquired from an understanding of the geologic features under study or directly from the computation of local dips in the coherent reflections found in the seismic data. In this study, the known LVA (Figure 2c) field is used in the computation of the experimental variogram from the true model (natural logarithm of the impedance). Subsequently, a parametric function that fits the experimental variogram was determined.

Table 1 summarizes the parametric models used in the computation of the covariance matrix for the respective cases. Dimensionless lag units are used to characterize locations in the the 2D grid in which estimates of the impedance are to be computed. Three quantitative methods are used to characterize the fitness to the "true" model: correlation coefficient of the estimated-true cross plots, root mean square error, and the variance of the estimated model parameters. The inversion process follows step (2) and the inverse of the wyllie petrophysical transform (Bosch, 2004) is used to obtain estimates of the porosity from the estimates of the impedance.

Table 1: Summary of parametric models used in the computation of model covariances for cases 2, 3, and 4.

	Parametric model	nugget	range	variance
Case 2	Exponential	0	a_{min}= a_{max}=1.6	Variance of $\log(\mathbf{Z}_p)$ at CDP=5
Case 3	Exponential	0	a_{max} = 100a_{min}; a_{min}=1.6 Major direction of continuity is along direction of increasing CDP number	Variance of $\log(\mathbf{Z}_p)$ at CDP=5
Case 4	Exponential	0	a_{min}= a_{max}=93 (Non Euclidean distance, Boisvert and Deutsch, 2011)	Variance of $\log(\mathbf{Z}_p)$ at CDP=5

Figures 5-8 show the results of the inversion for trace 1(CDP=1) in the respective cases when SNR=1. As expected, all cases provide smooth solutions. The 2D plots of the estimated impedance models (Figure 9) provide a better view for one to assess the quality of the fit in the respective cases. For a data set with SNR as low as 1, the results suggest that better prediction of the model parameters is achieved once coupling between the model parameters are accounted for within $\mathbf{C}_m$. The high correlation between the estimated model parameters and the true model as well as the high variance obtained when

the inversion is constrained by locally varrying anisotropy corroborate the importance of properly accounting for vertical and lateral correlation between model parameters (Figure 10).

We also performed tests using seismic data with SNR=10 (Figure 4c). Table 2 summarizes the results for all the cases in this study where the goodness of the prediction is assessed for trace 1 as well as for all the traces combined. Estimated 2D impedance models from the second test are shown in Figure 11. While the aspect of using LVA to constrain the vertical and lateral continuity between the model parameters improves the quality of the model estimates, the results in Table 2 indicate that the advantage is marginal with respect to the other scenarios when the signal to noise ratio is large (SNR >10).

Table 2: Standard deviation (STD) of the predicted impedance model parameters, root mean square errors (RMSE) and corresponding correlation (Corr) between the predicted and "true" impedance model parameters.

		CDP=1			All traces		
		Corr	RMSE (x 10^6 Kg/s m^2)	STD (x 10^6 Kg/s m^2)	Corr	RMSE (x 10^6 Kg/s m^2)	STD (x 10^6 Kg/s m^2)
SNR=1	Case 1	0.647	1.29	1	0.495	12	0.92
	Case 2	0.644	1.30	1.25	0.481	13.1	1.21
	Case 3	0.738	1.14	1.31	0.560	11.4	1.01
	Case 4	0.723	1.17	1.29	0.609	11.3	1.19
SNR=10	Case 1	0.872	0.824	1.49	0.787	8.36	1.14
	Case 2	0.872	0.832	1.63	0.772	8.78	1.23
	Case 3	0.893	0.759	1.52	0.809	7.97	1.18
	Case 4	0.887	0.777	1.52	0.826	7.70	1.23

b)   Discussion

In this study, the numerical tests have been solved using least squares methods. Although such methods may give local solutions, they however provide satisfactory results as demonstrated in this study. General solutions can be obtained by using monte carlo methods. Jensäs (2008) also used least squares optimization methods in order perform amplitude variation with angle (AVA) inversion. In order to obtain estimates of the velocities (P- and S- waves) and densities, Jensäs (2008) constrains the lateral continuity in the inversion by assuming markov properties whereby the inversion result on one trace is only dependent on neighbouring traces $i-1$ and $i+1$. The latter can also be viewed as conditional independence (Jensäs, 2008): given traces $i-1$ and $i+1$, the elastic parameters of trace i are independent of all other traces except for trace $i-1$ and trace $i+1$. Unfortunately, such approach makes no accommodation for local dips associated to the lateral continuity of the model parameters one wants to estimate. Although the parameter estimated in our study is different from Jensäs' (2008) work, we go a step further to impose lateral continuity constrains in the inverse problem such that information about the local dip variations associated to the model parameters are included in the computation of the model variance matrix. The elements of the covariance matrix are obtained from parametric model fits to experimental variogram computed from the true 2D model of the natural log of the impedance with consideration for the LVA field shown in Figure 2c (Boisvert and Deutsch, 2011). An initial inversion of the 2D impedance model whereby the parameters are considered to be independent can be used as hard data when the LVA field is used in the computation of the experimental variogram.

In most inversion problems, proper consideration for lateral continuity is important. Improper definition of the lateral continuity may introduce artifacts in the 2D image of the estimated model parameters. For example, zones where layers merge cannot be properly estimated if the constrain for lateral continuity does not account for dipping events (Jensäs, 2008). The results in Figures 9a-c and 11a-c highlight the pitfalls in the inversion when the constrains for lateral continuity are not properly defined: single trace-based inversion causes the lateral continuity to be punctuated by vertical stripes; assuming geometric anisotropy where the major direction of anisotropy is horizontal introduces layer-like features (e.g. between 0s and 0.01s – Figure 11-c) in the estimated 2D image that are not present in the true impedance model (Figure 2b). Another advantage for using the proper lateral continuity constrains is that

lateral variations in the estimated model parameters look more geologically realistic. This can be observed by comparing images for cases 1-3 against those obtained when the LVA approach is used (Case 4) irrespective of the SNR associated to the seismic data. Results from cases 1-3 fail to properly capture the lateral continuity of some of the layers as shown in the true model. Some of the artifacts in the inversion results can also be attributed to the strategy adopted in implementing the inversion. This is especially observed in the results obtained in case 3 (Figures 9c and 11c) where the inversion was conducted by using multiples of 15 traces. The size of the traces used can be directly correlated to the horizontal scale of the artifacts in the inversion. The choice of using subsets of the traces was to reduce computation time. A similar strategy was also adopted to obtain results for case 4. However, artifacts associated to the implementation strategy are virtually absent for the results in case 4. Based on these observations, we thus considered the implementation strategy to have negligible bearing in the overall assessment of our modeling results.

Conclusions

Using Bayesian theory, we modify the formulation of the general inverse problem commonly found in geophysical inversion. The formulation uses geostatistical tools to impose constrains on the lateral continuity of the model parameters. This is achieved by modifying the model covariance matrix such that its elements consist of covariances computed with consideration for locally varrying anisotropy (LVA). Least squares results obtained in this work corroborate that better geologically consistent prediction of the model parameters can be achieved when LVA is considered. Unfortunately, the main challenge in this method is in defining the LVA field. When knowledge of LVA exists, it should be incorporated in the seismic inversion process in order to improve the predictions of the model parameters of interest especially from seismic data with a low signal to noise ratio.

References

Buland, A., and H. Omre, 2003, Bayesian linearized AVO inversion: Geophysics, Vol. 68, pp 185-198, doi: 10.1190/1.1543206.

Bosch, M., Mukerji, T., and Gonzalez, E. F., 2010, Seismic inversion for reservoir properties combining statistical rock physics and geostatistics: A review: Geophysics, Vol. 75, pp 75A165-75A176.

Sacchi, M.D, Ulrych, T. J., and Walker, C. J., 1996, Interpolation and Extrapolation Using a High-Resolution Discrete Fourier Transform: IEEE Transactions on Signal Processing, Vol. 46, No. 1, pp 31-38.

Bosch, M., 2004, The optimization approach to lithological tomography: Combining seismic data and petrophysics for porosity prediction: Geophysics, Vol. 69, pp 1272-1282.

Velis, D. R., 2008, Stochastic sparse-spike deconvolution: Geophysics, Vol. 73, pp R1-R9.

Oldenburg, D. W., T. Scheuer, and S. Levy, 1983, Recovery of the acoustic impedance from reflection seismograms: Geophysics, 48, pp 1318-1337.

Bosch, M., C. Carvajal, J. Rodrigues, A. Torres, M. Aldana, and J. Sierra, 2009, Petrophysical seismic inversion conditioned to well-log data: Methods and application to a gas reservoir: Geophysics, Vol. 74, No. 2, pp O1-O15, doi: 10.1190/1.3043796.

Eidsvik, J., P. Avseth, H. Omre, T. Mukerji, and G. Mavko, 2004, Stochastic reservoir characterization using prestack seismic data: Geophysics, Vol. 69, pp 978-993, doi: 10.1190/1.1778241.

Torres-Verdin, C., M. Victoria, G. Merletti, and J. Pendrel, 1999, Trace-based and geostatistical inversion of 3$-$D seismic data for thin-sand delineation: An application in San Jorge basin, Argentina: The Leading Edge, Vol. 18, pp 1070-1077, doi: 10.1190/1.1438434.

Ulrych, T. J., M. D. Sacchi, and A. Woodbury, 2001, A Bayes tour of inversion: A tutorial: Geophysics, Vol. 66, pp 55-69, doi: 10.1190/1.1444923.

Jensäs I. O, 2008, A blockyness constraint for seismic AVA inversion, M.Sc Thesis, Norwegian University of Science and Technology.

Pendrel, J. V., and van Riel, P., 1997, Methodology for Seismic Inversion- A Western Canadian Reef Example: CSEG Recorder, Vol. 22, No. 5, p.5.

Tarantola, A., 2005, Inverse problem theory and methods for model parameter estimation: SIAM.

Alemie, W., and Sacchi, M. D., 2010, High-resolution three-term AVO inversion by means of a Trivariate Cauchy probability distribution: Geophysics, Vol. 76, No. 3, pp R43-R55.

Deutsch, C., and A. Journel, 1998, GSLIB: Geostatistical Software Library: Oxford University Press.

Goovaerts, P., 1997, Geostatistics for Natural Resources, Applied Geostatistics Series, Oxford University Press.

Doyen, P. M., 1988, Porosity from seismic data: A geostatistical approach: Geophysics, Vol. 53, pp 1263-1275.

Haas, A., and Dubrule, O., 1994, Geostatistical inversion- A sequential method of stochastic reservoir modeling constrained by seismic data: First Break, 12, pp 561-569.

Boisvert, J. B. and Deutsch, C. V., 2011, Programs for kriging and sequential Gaussian simulation with locally varying anisotropy using non-Euclidean distances: Computers & Geosciences, Vol. 37(4), pp 495-510.

Goff, J. A., and Jordan, T. H., 1988, Stochastic modeling of seafloor morphology: Inversion of Sea Beam data for second-order statistics, Journal of Geoph. Res., Vol. 93, pp 13,589-13,608.
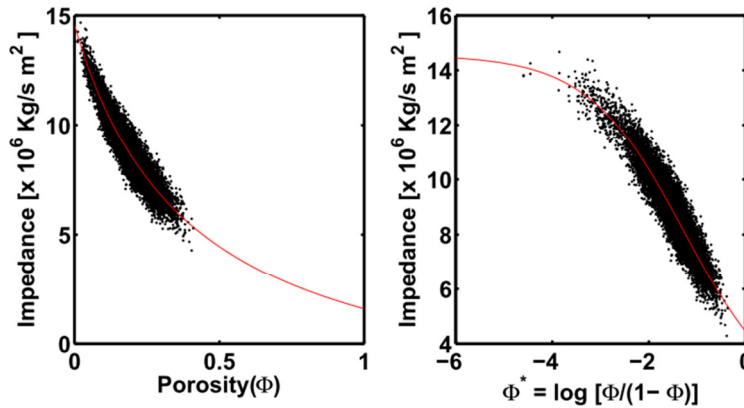
Figures

Figure 1: Cross plots of impedance and porosity for the 2D model. The line represents the wyllie petrophysical transform. $\log\left(\mathbf{Z}_p\right)$ is the parameter that is estimated during the inversion process ($\mathbf{Z}_p$ = Impedance).
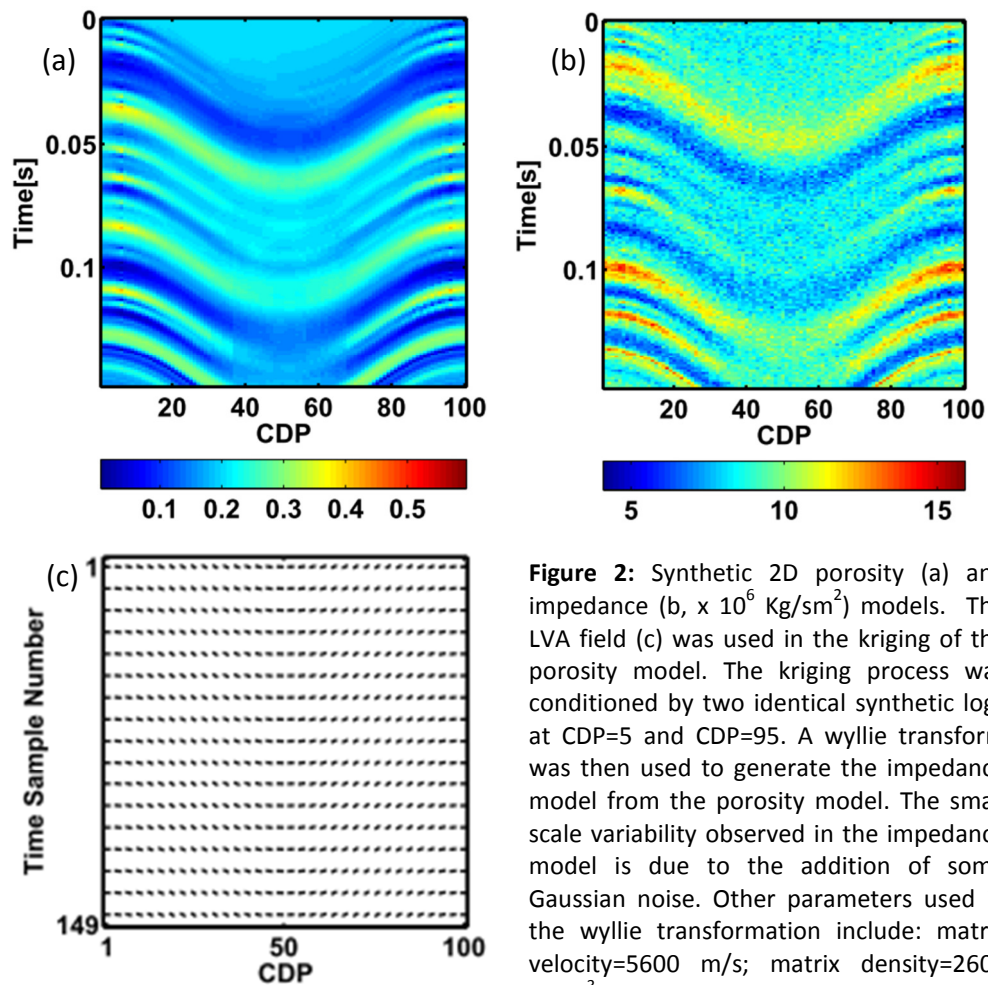

Figure 2: Synthetic 2D porosity (a) and impedance (b, x 10^6 Kg/sm^2) models. The LVA field (c) was used in the kriging of the porosity model. The kriging process was conditioned by two identical synthetic logs at CDP=5 and CDP=95. A wyllie transform was then used to generate the impedance model from the porosity model. The small scale variability observed in the impedance model is due to the addition of some Gaussian noise. Other parameters used in the wyllie transformation include: matrix velocity=5600 m/s; matrix density=2600 Kg/m^3; fluid velocity=1587 m/s; fluid density=1000 Kg/m^3 (Bosch, 2004).
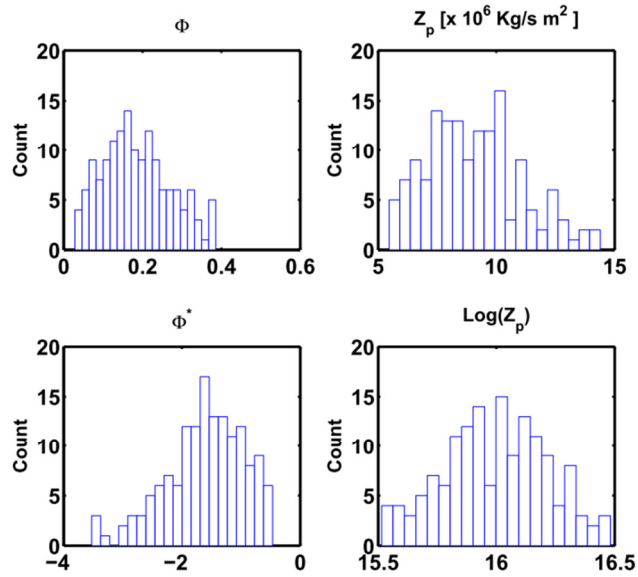
Figure 3: Histograms of the well logs at CDP=5. While the top row shows the porosity and impedance values, the bottom row shows natural log transformations of these variables. $\phi = \log\left(\phi/\left(1-\phi\right)\right)$.
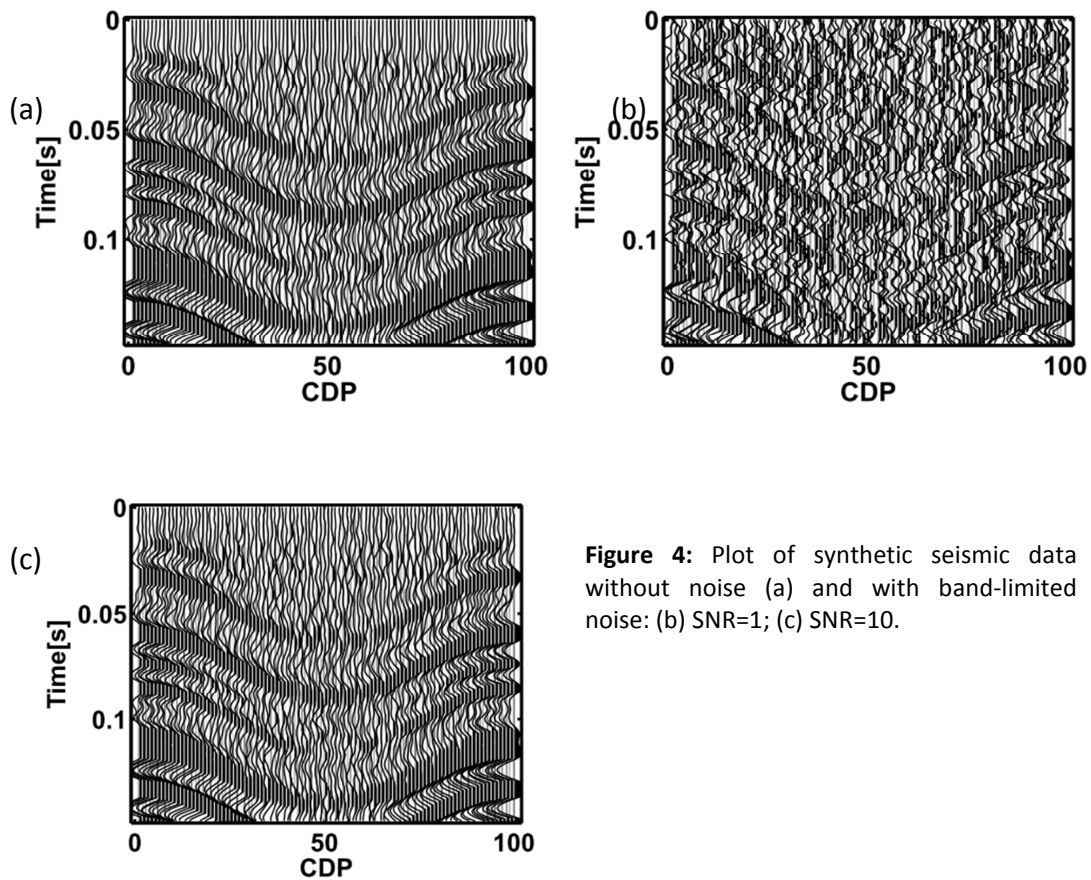
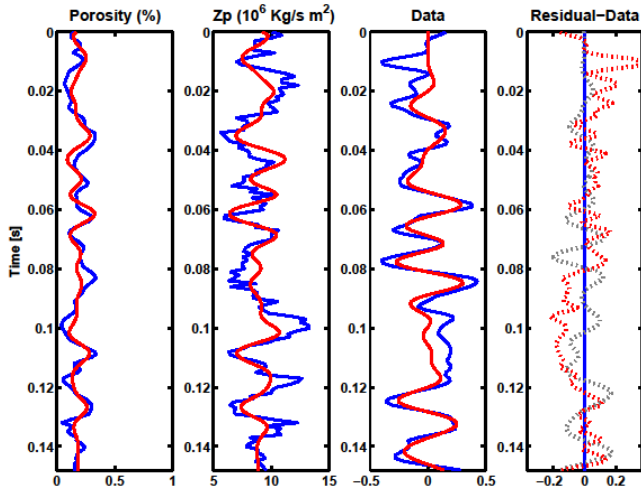**Figure 4:** Plot of synthetic seismic data without noise (a) and with band-limited noise: (b) SNR=1; (c) SNR=10.

Figure 5: 2D Inversion test (Case 1, SNR=1) showing true porosity-impedance models with its corresponding seismic data(blue), and the estimated porosity-impedance model with its corresponding seismic data (red) at CDP=1. The fourth panel compares the residual of the seismic data (red) with the noise (gray) present in the observed data. An inverse of the wyllie transform is used to map the estimated impedance model to porosity.
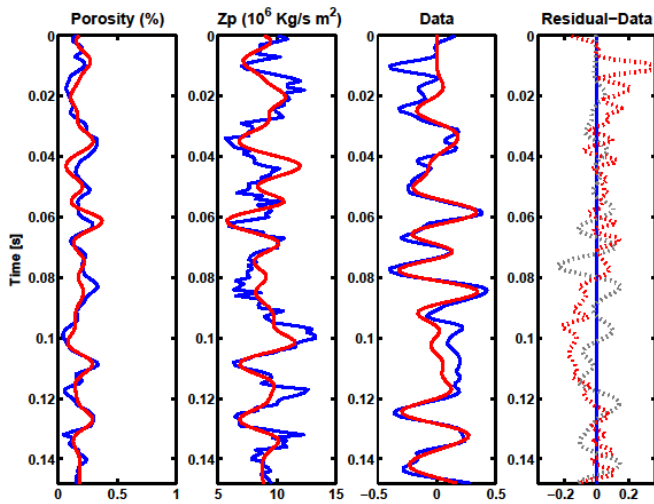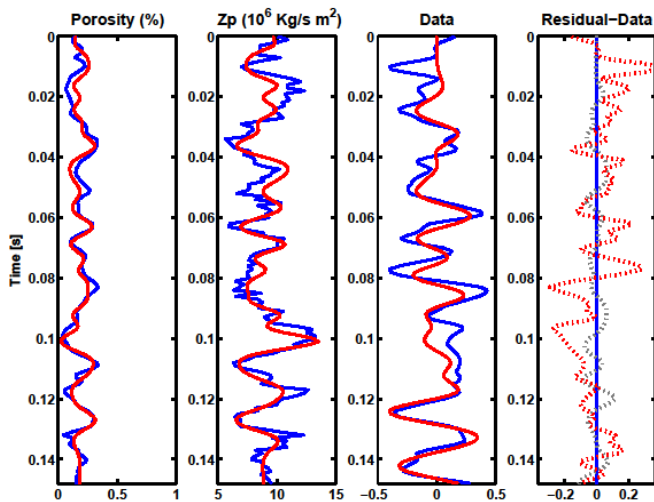

Figure 6: 2D Inversion test (Case 2, SNR=1) showing true porosity-impedance models with its corresponding seismic data(blue), and the estimated porosity-impedance model with its corresponding seismic data (red) at CDP=1. The fourth panel compares the residual of the seismic data (red) with the noise (gray) present in the observed data. An inverse of the wyllie transform is used to map the estimated impedance model to porosity.
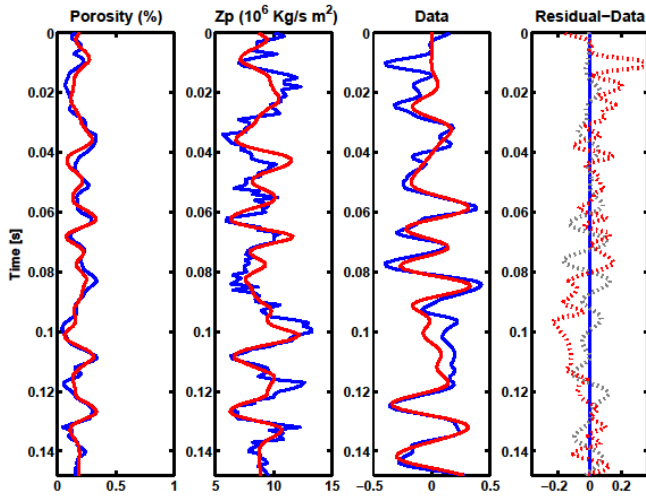

Figure 7: 2D Inversion test (Case 3, SNR=1) showing true porosity-impedance models with its corresponding seismic data(blue), and the estimated porosity-impedance model with its corresponding seismic data (red) at CDP=1. The fourth panel compares the residual of the seismic data (red) with the noise (gray) present in the observed data. An inverse of the wyllie transform is used to map the estimated impedance model to porosity.

Figure 8: 2D Inversion test (Case 4, SNR=1) showing true porosity-impedance models with its corresponding seismic data(blue), and the estimated porosity-impedance model with its corresponding seismic data (red) at CDP=1. The fourth panel compares the residual of the seismic data (red) with the noise (gray) present in the observed data. An inverse of the wyllie transform is used to map the estimated impedance model to porosity.
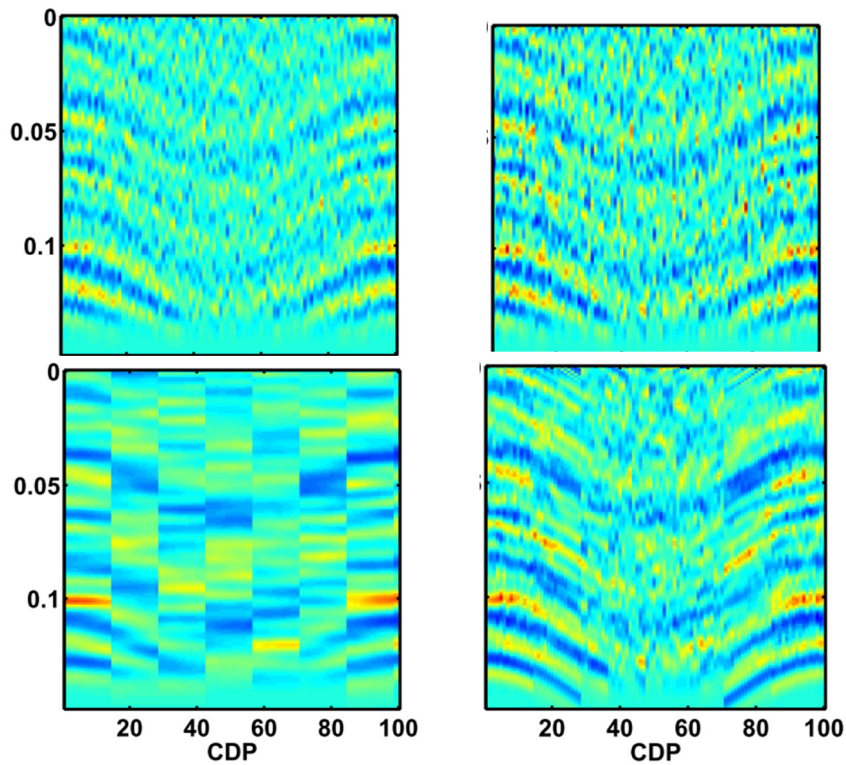
Figure 9: 2D Inversion results for the impedance (10^6 Kg/s m^2, SNR=1): (a) CASE 1- model parameters are independent; (b) CASE 2- model parameters are correlated in the vertical direction (time axis); (c) CASE 3- correlation in the model parameters is characterized by geometric anisotropy where the maximum direction of continuity is horizontal;
(d) CASE 4- correlation in the model parameters uses anisotropic distances that take the LVA field in to account.
Clearly, the results in (c) show features that are the least consistent with those observed in the "true" model (Figure 2b). The color scales in these plots are identical to the one used in Figure 2b.
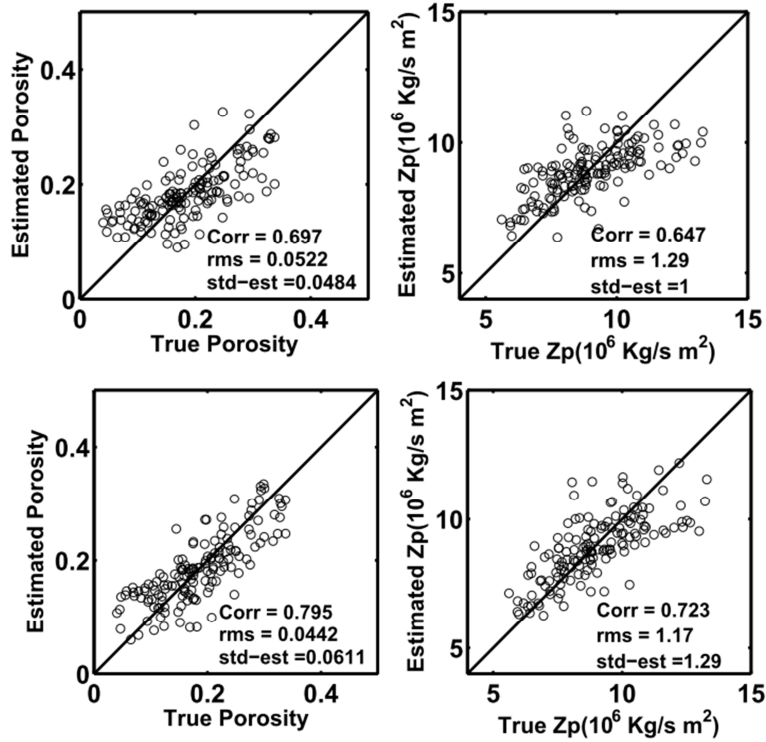
Figure 10: Cross plots comparing "true" with "estimated" impedance model parameters at CDP=1: *top row*- CASE 1 (model parameters are independent); *bottom row*- CASE 4 (correlation in the model parameters uses anisotropic distances that take the LVA field in to account). An inverse of the wyllie transform is used to map the estimated impedance model to porosity.
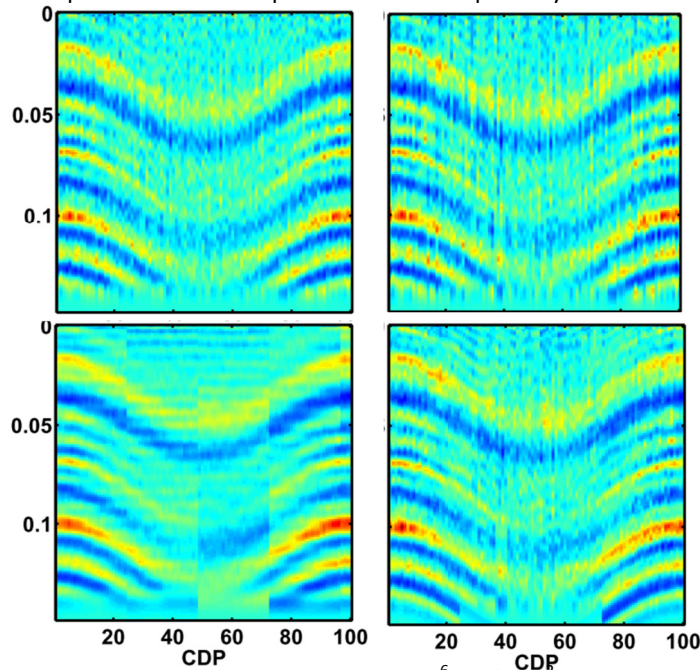

Figure 11: 2D Inversion results for the impedance (10^6 Kg/s m^2, SNR=10): (a) CASE 1- model parameters are independent; (b) CASE 2- model parameters are correlated in the vertical direction (time axis); (c) CASE 3- correlation in the model parameters is characterized by geometric anisotropy where the maximum direction of continuity is horizontal; (d) CASE 4- correlation in the model parameters uses anisotropic distances that take the LVA field in to account. The color scales in these plots are identical to the one used in Figure 2b.